Check for updates

JGR Atmospheres

RESEARCH ARTICLE
10.1029/2021JD034614

Seasonality in Saharan Dust Across the Atlantic Ocean: From Atmospheric Transport to Seafloor Deposition

Michèlle van der Does[1,2], Geert-Jan A. Brummer[1], Laura F. Korte[1], and Jan-Berend W. Stuut[1,3]

[1]Department of Ocean Systems, NIOZ – Royal Netherlands Institute for Sea Research, Texel, The Netherlands, [2]Helmholtz Centre for Polar and Marine Research, Department of Marine Geology, Alfred Wegener Institute, Bremerhaven, Germany, [3]Department of Earth Sciences, Faculty of Science, Vrije Universiteit Amsterdam, The Netherlands

Key Points:

- First time series of bi-weekly dust concentrations measured *in situ* across the remote Atlantic
- Dust deposition fluxes and grain size peak in summer and/or autumn, with wet deposition dominating total dust deposition and seasonal trends
- Large differences in dust characteristics exist between transport and deposition, while rain deposits more and coarser dust

Correspondence to:
M. van der Does,
michelle.van.der.does@awi.de

Citation:
van der Does, M., Brummer, G.-J. A., Korte, L. F., & Stuut, J.-B. W. (2021). Seasonality in Saharan dust across the Atlantic Ocean: From atmospheric transport to seafloor deposition. *Journal of Geophysical Research: Atmospheres*, *126*, e2021JD034614. https://doi.org/10.1029/2021JD034614

Received 18 JAN 2021
Accepted 17 MAY 2021

© 2021. The Authors.
This is an open access article under the terms of the Creative Commons Attribution-NonCommercial-NoDerivs License, which permits use and distribution in any medium, provided the original work is properly cited, the use is non-commercial and no modifications or adaptations are made.

Abstract Saharan dust is transported in great quantities from the North African continent every year, most of which is deposited across the North Atlantic Ocean. This dust impacts regional and global climate by affecting the atmospheric radiation balance and altering ocean carbon budgets. However, little research has been carried out on time series of Saharan dust collected *in situ* across the open Atlantic. Here, we present a unique three-year time series of Saharan dust along a trans-Atlantic transect, sampled by moored surface buoys and subsurface sediment traps. Results show a good correlation between the particle-size distributions of atmospheric dust and the lithogenic particles settling to the deep ocean floor, confirming the aeolian origin of the lithogenic particles intercepted by the subsurface sediment traps, even in the distal western part of the Atlantic Ocean. Dust from both dry and wet deposition as collected by the sediment traps, shows increased deposition fluxes and coarser grain size in summer and/or autumn that coincides with increased precipitation at the sampling sites as derived from satellite data. In contrast, both buoys that sampled dust during transport at sea level show little seasonal variation in both concentration and particle size, as the large amounts of dust transported in summer and early autumn at high altitudes are far above their sampling range. This implies that wet deposition in summer and autumn defines the typical seasonal trends of both the dust deposition flux and its particle-size distribution observed in the sediment traps.

1. Introduction

Saharan dust is exported in large quantities from the African continent and transported across the Atlantic Ocean toward the Caribbean. Estimates amount to 136–222 Tg annually (H. Yu et al., 2019), although this may well be an underestimation (Adebiyi & Kok, 2020). This atmospheric dust can alter radiation budgets (Ryder et al., 2019) and can act as cloud condensation and ice nuclei (Atkinson et al., 2013; Twohy et al., 2009). Dust deposited in the ocean delivers nutrients, which in turn enhance the ocean's carbon cycle as they stimulate phytoplankton growth (Mills et al., 2004; Pabortsava et al., 2017). Large dust particles can subsequently enhance carbon export to the ocean floor by acting as mineral ballast particles that accelerate settling of organic matter aggregates (Pabortsava et al., 2017; Van der Jagt et al., 2018).

Dust emissions from northwest Africa show a large inter-annual variability, and the amount of dust deposition decreases with increasing distance from the source (Goudie & Middleton, 2001; Van der Does et al., 2020). Dust particles are removed from the atmosphere by both dry and wet depositional processes (Bergametti & Forêt, 2014; Zender et al., 2003). Wet deposition of dust potentially increases the bio-availability of nutrients carried with the dust particles (Korte et al., 2018; Meskhidze et al., 2005), that can lead to an increased fertilization effect of dust deposition in the oceans (Ridame et al., 2014). The size of the emitted dust particles is determined by conditions at the source, such as dust-source availability, wind velocity, erosion threshold, and soil particle size (Marticorena, 2014). Subsequently, the particle size of deposited dust over the ocean is related to the distance from the source, with dust deposited at proximal locations being coarser-grained than dust deposited at distal locations (Holz et al., 2004; Sarnthein et al., 1981; Van der Does et al., 2016).

Saharan dust transport and deposition were previously studied on continental Africa (Friese et al., 2017; Kandler et al., 2009; Marticorena et al., 2010; Skonieczny et al., 2013), in the eastern part of the North Atlantic

Ocean (Bory et al., 2002; Brust et al., 2011; Fischer et al., 2016; Friese et al., 2016; Sarnthein et al., 1981), or in the Caribbean and North and South America (Prospero et al., 2010, 2014; H. Yu et al., 2015). These observations have provided important and long-term records of Saharan dust deposition. However, these are mostly based on a small region in the ocean or on land. Atmospheric dust has also been sampled over and across the Atlantic Ocean during airplane campaigns (Ryder et al., 2019; Weinzierl et al., 2017) and shipboard expeditions (Baker et al., 2010; Stuut et al., 2005). However, these measurements represent snapshots in time. The combined results from these studies show that dust deposition peaks in winter in the east, close to the northwest African sources of the dust (Fischer et al., 2016; Fomba et al., 2014; Skonieczny et al., 2013), and in summer in the west, at distal sites in the Caribbean (Prospero et al., 2014). Satellite observations reveal largest interannual variability in spring and smallest in summer (H. Yu et al., 2019). The seasonality can be partly attributed to the latitudinal movement of the Intertropical Convergence Zone (ITCZ), influencing the prevailing dust-transporting wind systems (Adams et al., 2012; Ben-Ami et al., 2012; Nicholson, 2000; H. Yu et al., 2019). The Saharan Air Layer (SAL) transports the dust between 5 and 7 km in summer, as opposed to the Harmattan winds that transport the dust at lower altitudes (0–3 km) in winter (Adams et al., 2012; Muhs, 2013; Stuut et al., 2005; Tsamalis et al., 2013).

In situ time-series observations of dust deposition across the entire Atlantic Ocean are sparse, and therefore a unique long-term sampling campaign was started in 2012. This transect consisted of subsurface sediment traps along a transect from east to west at 12°N, directly underneath the main path of the Saharan dust plume (e.g., Van der Does et al., 2016). Previous results of this transect are summarized in Section 3.1 below. The sediment traps collect dust during its descent from surface ocean toward the ocean floor, which can be several days up to weeks after deposition on the surface ocean. To get more information about the characteristics of Saharan dust after its trans-Atlantic transport, we sampled directly from the atmosphere close above the ocean surface with tethered surface buoys. This allows the comparison between dust during transport and dust after deposition, and the characterization of the changes the dust undergoes during dry and wet deposition and while settling to the ocean floor.

Here we present unique data of more than two years of atmospheric dust concentrations and dust particle size at two of the stations of the transect, collected from the atmosphere by moored surface buoys as well as passive air samplers. In addition, we expand the existing records of dust particle size and dust deposition fluxes from the sediment traps along the Atlantic transect. This comprehensive data set provides important insights into magnitudes and changes of dust transport and deposition across the Atlantic Ocean, and especially the evolution of dust characteristics from transport to deposition. It is a unique combination of extensive spatial coverage from source to sink, as well as a continuous record over multiple years. This continuous data set of dust concentration, dust deposition fluxes and grain size along a transect in the remote open ocean will be useful for validating and constraining model simulations with various complexity, from fully coupled Earth system models (Kok et al., 2020) to simple deposition-enabled trajectory models (Y. Yu et al., 2020).

2. Material and Methods

Saharan mineral dust was sampled between October 2012 and March 2016 along a trans-Atlantic transect at 12°N (Figure 1a), using three sampling methods. At five sites (M1–M5), dust was collected by sediment traps moored at 1,200 and 3,500 m below the sea surface (below sea level - bsl; Figures 1b and 1c). For the second sampling year, 2014, the transect was expanded with two surface buoys, moored at two stations in the center of the transect (M3 and M4), that sampled dust *in situ* directly from the atmosphere. These buoys were equipped with 24 sample filters actively filtering the air. Both buoys were additionally equipped with a passive air sampler (MWAC – Modified Wilson and Cooke; Goossens & Offer, 2000). This unique combination of different sampling methods delivers new insights into dust transport and deposition processes across the Atlantic, while the multi-year record allows for the identification of seasonal and inter-annual variability.

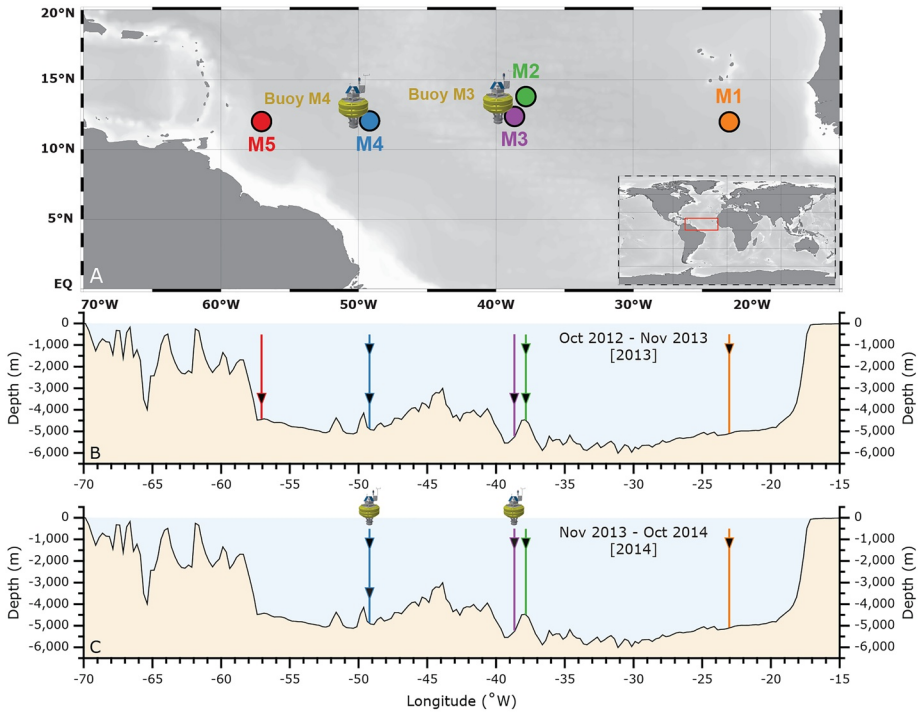

Figure 1. Set-up of trans-Atlantic dust sampling. (a) Sampling locations with sediment traps at stations M1–M5 and moored surface buoys at M3 and M4. The map was created using Ocean Data View (Schlitzer, 2018). (b and c) Bathymetry along 12°N (source: gebco.net) with successful sediment-trap sampling of the 2013 and 2014 sampling series and surface buoys in 2014. In 2015 the surface buoys continued for a second year (not shown).

2.1. Sediment Traps

Sediment traps were moored at five stations along a transect across the Atlantic Ocean, as described by Van der Does et al. (2016) and Korte et al. (2017). Four moorings were located at ~12°N, and a fifth at ~14°N (Figure 1a). Sediment traps were located at 1,200 m (upper, or U) and 3,500 m (lower, or L) below the ocean surface on each mooring. The traps contained 24 sampling bottles, pre-programmed to synchronously sample over 8 and 16-day intervals (Table 1). During the first year (2013), the traps sampled from October 19, 2012 to November 7, 2013 at all five sites (henceforth called 13M1–13M5), at 16-day intervals. During the second year (2014), the traps sampled from November 23, 2013 until October 25, 2014 at M1–M4 (henceforth called 14M1–14M4), at 8- and 16-day intervals. This variable sampling resolution was applied to minimize sampling gaps and to synchronize sediment-trap sampling at all stations. The recovery was slightly different for the two sampling years, with seven sediment traps recovered after the first sampling year, and five after the second sampling year (Figures 1b and 1c). Detailed information on the mooring equipment and exact sampling intervals is given in the respective cruise reports (Stuut et al., 2012, 2013, 2015). For 14M1-U only the first nine samples out of 24 could be recovered due to a rotation malfunction of the trap carrousel. Sediment-trap sample preparation is described in more detail by Van der Does et al. (2016, 2020). In brief, a biocide was added to the sampling bottles ($HgCl_2$, 1.3 g L^{-1}) and a pH buffer (borax; $Na_2B_4O_7 \cdot 10H_2O$, 1.3 g L^{-1}, pH ≈ 8) that created a density slightly higher than the ambient seawater to prevent the solution diffusing out of the bottles. After recovery, samples were wet-sieved through a 1 mm mesh and subsequently split into 1/5 and 1/25 aliquots using a WSD10 rotary splitter (McLane Laboratories, USA). The average weight difference between replicate 1/5 splits is 2.7% (SD = 2.4), with 84% of all samples having a weight difference of <5% between splits.

A mid-date was assigned to each sample interval, which is the middle of their 8 or 16-day sampling periods. The samples were grouped into seasons: autumn (SON), winter (DJF), spring (MAM), and summer (JJA). Organic aggregates in which dust particles are incorporated have average settling velocities of about 200 m day^{-1} (Nowald et al., 2015), although much higher settling velocities up to 400 m day^{-1} can be reached

Table 1
Sampling Positions, Intervals, Average Particle Size and Dust Content (Deposition Flux or Dust Concentration) of Sediment Traps of 2013 (13M1–M5) and 2014 (14M1–M4), Buoys of 2014 (M3-A and -B, M4-A) and 2015 (M3-C and M4-C), and MWAC Samplers of 2014 and 2015

Sampler	Lat. (°N)	Lon. (°W)	Trap depth (m bsl)	km to African coast	Sampling intervals	Sampling period	Avg. modal grain size	Avg. dust content
13M1	12.00	23.00	1,150	700	16 days	October 19, 2012–November 7, 2013	18.25 μm	14.27 mg $m^{-2}d^{-1}$
13M2	13.81	37.82	1,235; 3,490	2,300	16 days	October 19, 2012–November 7, 2013	13.85 μm	3.11 mg $m^{-2}d^{-1}$
13M3	12.39	38.63	3,540	2,400	16 days	October 19, 2012–November 7, 2013	16.47 μm	4.64 mg $m^{-2}d^{-1}$
13M4	12.06	49.19	1,130; 3,370	3,500	16 days	October 19, 2012–November 7, 2013	10.39 μm	3.72 mg $m^{-2}d^{-1}$
13M5	12.02	57.04	3,520	4,400	16 days	October 19, 2012–November 7, 2013	6.99 μm	8.69 mg $m^{-2}d^{-1}$
14M1	12.00	23.01	1,200	700	8 and 16 days	November 23, 2013–March 31, 2014	15.20 μm[a]	9.46 mg $m^{-2}d^{-1}$ [a]
14M2	13.81	37.82	1,190	2,300	8 and 16 days	December 1, 2013–October 25, 2014	13.35 μm	2.86 mg $m^{-2}d^{-1}$
14M3	12.40	38.63	1,362	2,400	8 and 16 days	December 1, 2013–October 17, 2014	12.85 μm	3.66 mg $m^{-2}d^{-1}$
14M4	12.04	49.22	1,110; 3,316	3,500	8 and 16 days	December 9, 2013–October 25, 2014	11.10 μm	2.40 mg $m^{-2}d^{-1}$
Buoy 2014 M3-A	~12.3	~38.7	-	2,400	8 and 16 days	December 1, 2013–April 20, 2014	-	-
Buoy 2014 M3-B	~12.3	~38.7	-	2,400	8 days	September 7, 2014–January 21, 2015	-	-
Buoy 2015 M3-C	~12.3	~38.7	-	2,400	11 and 22 days	January 26, 2015–March 29, 2016	19.9 μm	0.0198 μg L air^{-1}
Buoy 2014 M4-A	~12.0	~49.1	-	3,500	15–16 days	December 9, 2013–March 30, 2014	-	-
Buoy 2015 M4-C	~12.0	~49.1	-	3,500	11 and 22 days	February 6, 2015–March 21, 2016	24.2 μm	0.0082 μg L air^{-1}
MWAC 2014 M3	~12.3	~38.8	-	2,400	Continuously (281 days)	November 24, 2013–September 1, 2014	8.54 μm	0.05 mg day^{-1}
MWAC 2014 M4	~12.0	~49.1	-	3,500	Continuously (425 days)	November 28, 2013 –January 27, 2015	11.29 μm	0.04 mg d^{-1}
MWAC 2015 M3	~12.3	~38.8	-	2,400	Continuously (434 days)	January 22, 2015–March 31, 2016	12.4 μm	0.13 mg d^{-1}
MWAC 2015 M4	~12.0	~49.1	-	3,500	Continuously (422 days)	January 28, 2015–March 25, 2016	10.29 μm	0.07 mg d^{-1}

Abbreviation: MWAC, Modified Wilson and Cooke.
[a]Average of nine samples.

during high dust deposition conditions (Van der Jagt et al., 2018). Therefore, we assume an average delay of 6 days for the aggregates to settle from the ocean's surface to the sediment traps at 1,200 m depth, and another 11.5 days to the sediment traps at 3,500 m depth, after initial residence in the surface waters (Brust et al., 2011). This agrees with previously determined settling velocities for these sediment-trap samples of >140 m per day (Korte et al., 2017; Van der Does et al., 2016).

2.2. Buoys and MWAC Samplers

In conjunction with the sediment traps, two dust-collecting surface buoys were moored at sampling stations M3 and M4, respectively (Figure 1). Such time series of in situ atmospheric dust observations over the remote tropical Atlantic Ocean are unique in its kind. The buoys were first deployed in November 2013 (Buoys M3-A and M4-A; Stuut et al., 2013), subsequently re-deployed in 2014 and 2015 (Buoy M3-B; Bale, 2014; and Buoys M3-C and M4-C; Stuut et al., 2015), and recovered in 2016 (Stuut et al., 2016). The buoys were built at NIOZ, based on the aerosol-collecting buoys designed by E. Sholkovitz (e.g., Sholkovitz & Sedwick, 2006; Sholkovitz et al., 2001), and are still being developed (Figure 2). The buoys consist of a carrousel with 24 filters which rotate under the air inlet, synchronously with the subsurface sediment traps below the buoys at 8 to 22-day sample intervals (Table 1). The buoys collect aerosols by pumping air through the 47 mm polycarbonate filters of 0.2 μm pore size. These aerosols predominantly consist of mineral dust but also inevitably contain variable amounts of sea salts from spray. The volume of air filtered by the sampler is monitored, and the buoys are linked to a meteorological sensor that monitors wind speed, wind direction, temperature, precipitation and relative humidity, which allows the buoys to only sample under favorable weather conditions, i.e., no precipitation (<0.2 mm min^{-1}) or strong winds (<20 m s^{-1}). Under

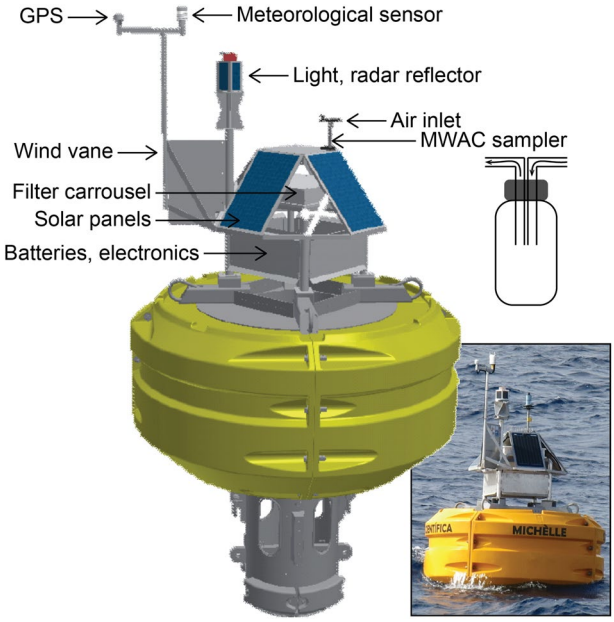

Figure 2. Details of the dust-collecting buoy and Modified Wilson and Cooke (MWAC) sampler.

these conditions, sampling was carried out once daily starting at 10:00 UTC for two hours (in 2014) or four hours (in 2015). If weather conditions were not favorable, the air inlet did not open while the weather kept being monitored for a period of eight hours. When weather conditions then changed to favorable for at least one hour, the sampling scheme was initiated. When the weather conditions changed to unfavorable conditions during sampling the schedule was aborted for another hour until another period of favorable conditions, limited to 18:00 UTC. The buoys are also equipped with a wind vane to keep the air inlet facing the wind, which was mostly blowing from an easterly direction. In addition, the buoys contain a satellite communications system (Iridium) that allows two-way communication.

In 2014, all buoy filters were recovered broken. Consequently, the dust concentration for the 2014 filters could not be determined, and not all broken filters contained sufficient material for particle-size analysis. The filters that did contain enough material for particle-size analysis may yield unreliable results due to the loss of coarse dust particles when the filter broke, and subsequent under-sampling. The dust collectors were modified for the second deployment in 2015, which included an additional acetate support filter underneath the sample filters, and a buffer chamber in the air-flow line to reduce oscillations of the filter caused by the membrane pump (Stuut et al., 2015). The volume of air sampling was also increased for the second year, as the first year revealed that the solar panels supplying power to the pumps worked very efficiently. After the second year of sampling (2015), all filters returned intact, and dust particle size and dust concentration could be determined. For each filter, an average of 2288 and 5914 L of air was sampled per day by buoys M3-C and M4-C, respectively, and each session the volume decreased as the filter became increasingly clogged by dust and sea salt. Since a larger volume of air was sampled per day for buoy M4, the engine must have sucked air through the filters at higher power, which could have influenced the collection of (large) dust particles. Due to technical problems with the power supplies of the buoys, the entire sampling schedule was not completed for every deployment.

In addition to the filters, both buoys were equipped with an MWAC sampler (Modified Wilson and Cooke; Goossens & Offer, 2000), a passive air sampler that sampled continuously over the time the buoys were deployed (Table 1). The sampling periods for the MWAC samplers ranged between 281 and 434 days (Table 1), which may have biased the particle size of the entire sample. The MWAC sampler consists of a plastic bottle which acts as settling chamber, and is connected to an inlet and outlet tube of 7.5 mm diameter (Figure 2). The samplers were installed vertically on the buoy's air inlet. The buoy's wind vane ensured continuous windward orientation of the MWAC's inlet tube. The samplers were located about 3 m above sea level (Figure 2). These MWAC samplers have very high sampling efficiencies, between 75% and 105% for dust with a median particle size of 30 μm at wind velocities between 1 and 5 m s^{-1} (Goossens & Offer, 2000). Average wind velocity as recorded by buoy M3 (A–C) ranged between 4.1 and 9.9 m s^{-1} per sampling interval, with maximum velocities up to 18.3 m s^{-1}, well below the pre-set upper wind limit of 20 m s^{-1} for the buoys. For buoy M4 wind-velocity data are largely unavailable due to a technical failure of the electronics: for buoy M4-A wind velocities were recorded only for the first seven filters with large parts of the data missing, and for buoy M4-C no data were recorded at all. Sampling efficiency varies slightly with different wind speeds, but without apparent trends (Goossens & Offer, 2000). For sand-sized particles (median grain size of 132–287 μm), the efficiency reported in literature is slightly higher (90%–120%), but constant and independent of wind speed, for velocities between 6.6 and 14.4 m s^{-1} (Goossens et al., 2000).

2.3. Grain-Size Analysis and Dust Masses

For grain-size analysis of the subsurface sediment-trap samples, a 1/25 aliquot of the original sample was used. Prior to grain-size and flux analysis, all biogenic constituents were chemically removed from the

sediment trap samples to isolate the dust fraction (Van der Does et al., 2016). In short, organic matter was removed by adding 10 mL H_2O_2 (35%), carbonates using 10 mL HCl (10%) and biogenic silica with 6 g NaOH pellets in 100 mL of sample solution in demineralized water. After particle-size analysis the sediment-trap samples were filtered over pre-weighed 25 mm ∅, 0.4 μm pore size polycarbonate filters, rinsed with Milli-Q water, and subsequently weighed again to obtain the dust mass >0.4 μm and therefore the deposition flux (Van der Does et al., 2020). The average weight difference between replicate 1/5 splits of each sample is 2.7% (SD = 2.4), with 84% of all samples having a weight difference of <5% between splits. The highest deviation was found to be 13.6% (Van der Does et al., 2020).

Besides mineral dust, the buoy filters contained significant amounts of sea salt, which had to be removed from the filters before analyses. The original 47 mm ∅, 0.2 μm pore size polycarbonate buoy filters were ashed in a low-temperature asher and subsequently washed with Milli-Q water onto pre-weighed filters (25 mm ∅, 0.4 μm pore size polycarbonate), dried and weighed again to obtain the mass of the dust fraction >0.4 μm. Next, the filters containing the dust were ashed again in order to retrieve the dust particles for particle-size analysis. Although some of the buoy samples collected in 2013 did not contain sufficient material for reliable particle-size distributions, they did for $N = 6$ filters in M3-A, $N = 3$ in both M3-B and M4-A, $N = 14$ in M3-C and $N = 20$ in M4-C.

The MWAC samples only required the rinsing of the dust from the sample bottle with Milli-Q water prior to grain-size analysis, at the same time dissolving the present sea salts. After particle-size analysis these samples were also filtered and weighed on 47 mm ∅, 0.4 μm pore size (2014-MWACs) and 0.2 μm pore size (2015-MWACs) polycarbonate filters to establish long-term-averaged dust mass. Grain-size distributions of the MWAC samples were published by (Van der Does, Knippertz, et al., 2018).

Immediately prior to grain-size analysis of all samples, sodium pyrophosphate ($Na_4P_2O_7 \cdot 10H_2O$) was added to disaggregate the particles. Particle-size distributions were obtained using a Coulter laser diffraction particle sizer (LS13 320), equipped with a micro liquid module (MLM), as described by Van der Does et al. (2016). A magnetic stirrer homogenized the sample during analysis, and degassed water minimized the influence of air bubbles on the measurements. This resulted in particle-size distributions in the range of 0.375–2000 μm, divided into 92 size classes. This way, both the particle-size analyses and deposition fluxes are of the same dust size fraction >0.4 μm. Reproducibility experiments as described by Van der Does et al. (2016) with internal glass-bead standards reveal that the reproducibility is better than 0.7 μm for the mean and 0.6 μm for the median particle size (1σ). The average standard deviation integrated over all size classes is better than 4 vol.%.

2.4. Aerosol Optical Depth (AOD) and Precipitation

Aerosol optical depth (AOD) and precipitation data at the buoy sampling sites M3 and M4 were obtained at a daily resolution from the Moderate Resolution Imaging Spectroradiometer (MODIS) Terra satellite and Tropical Rainfall Measuring Mission (TRMM), for 1 × 1° boxes around the sampling sites. This was done through the Giovanni online data system, developed and maintained by the NASA GES DISC. For smoothing purposes, a 10-day running average was calculated.

3. Results

3.1. Previous Results of This Transect

Previous analyses of dust deposited on the seafloor and in subsurface sediment traps along the trans-Atlantic transect have been reported previously and are briefly summarized here. Dust particle sizes of the first year of sampling (2013), as well as seafloor sediments from all stations, were presented by Van der Does et al. (2016). These results showed a strong down-wind decrease in particle size, related to a decreasing contribution of large quartz particles and an increase of small clay minerals to the west (Korte et al., 2017). Dust deposition fluxes showed a similar downwind trend, with a significant decrease of dust deposition flux down-wind of the North African sources (Van der Does et al., 2020) for the upper (1,200 m) sediment traps for the first two years of sampling (2013 and 2014). Furthermore, the first two years of sampling revealed a distinct seasonal pattern of coarser dust particles deposited in summer (Van der Does et al., 2016) and

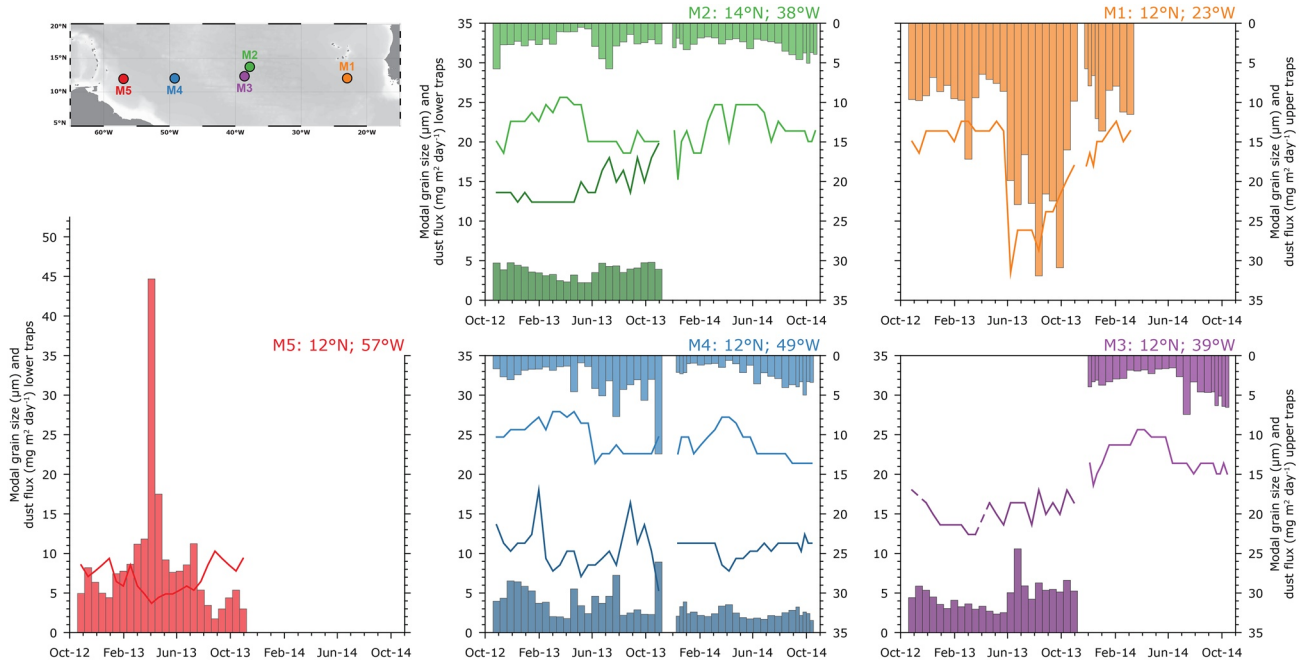

Figure 3. Modal grain sizes (lines) and dust deposition fluxes (bars) in the sediment traps of 2013–2014. The upper traps (1,200 m) are shown at the top of the graphs (right Y-axis has been inverted to ease comparison), and the lower traps (3,500 m) at the bottom (left Y-axis). Grain sizes of the first year of sampling (2013) and deposition fluxes of all upper traps were previously published in Van der Does et al. (2016, 2020).

at the same time increased deposition fluxes as a result of wet deposition (Van der Does et al., 2020). Wet deposition of dust is thought to enhance the bioavailability of carried nutrients (Korte et al., 2018), thereby providing a fertilizer enhancing productivity of e.g., calcifying phytoplankton (coccolithophores) as found in the sediment traps (Guerreiro et al., 2017). Grain-size distributions of the MWAC samples were published in Van der Does, Knippertz, et al. (2018), who also showed the long-range transport of giant (>75 µm) dust particles over thousands of kilometers.

In the current study, the gaps in the existing records have been filled and the records and time series have been extended to cover three consecutive years. In this study we add dust deposition fluxes of the lower sediment traps (3,500 m) of the first two years of sampling (2013 and 2014), as well as grain-size distributions of the second sampling year (2014). We also present the unique and novel results of time series of two dust-collecting surface buoys, that collect dust during transport just before it is deposited into the ocean.

3.2. Sediment-Trap Samples

Dust deposition along the transect is characterized by both downwind as well as seasonal trends. The newly obtained data of the second year of sampling (November 2013–October 2014) show a similar downwind fining as for the first year, with coarser particles deposited closer to the source at the easternmost sediment trap at M1 (23°W), and finer-grained particles westwards over greater distances (Figure 3). Dust deposition along the transect is also characterized by a downwind decrease, as most dust is deposited at the easternmost station M1, closest to the west African coast and the Saharan source (Figure 3; Van der Does et al., 2020). This downwind trend was also demonstrated by Korte et al. (2017), who showed that quartz particles, which are generally coarser and heavier than clay minerals, are predominantly deposited at proximal sites.

The seasonal signal of dust deposition shows more and coarser dust particles deposited in the sediment traps in summer and autumn, and less and finer particles in winter and especially in spring (Figure 3). This was also observed with satellite observations, showing largest dust deposition over the Atlantic Ocean in summer (H. Yu et al., 2019).

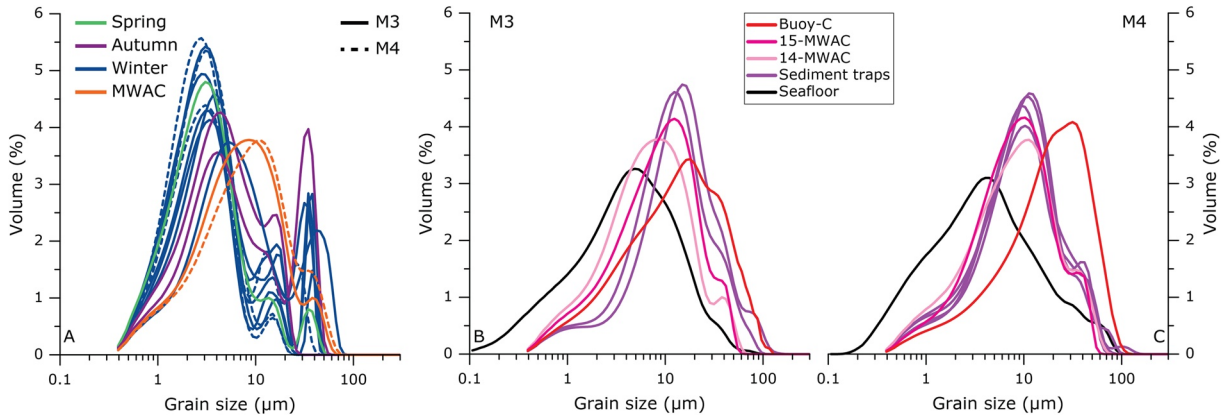

Figure 4. (a) Grain-size distributions of 2014 buoy filters of M3-A & B (solid lines) and M4-A (dashed lines), and 2014 Modified Wilson and Cooke (MWAC) samples from buoys M3 and M4 (orange lines). Each line represents an individual sample. (b and c) Average grain-size distributions of 2015 buoy-C filters, 2014 and 2015 MWAC samples, sediment traps (2013 and 2014 upper and lower traps) and seafloor sediments, from station M3 (b) and M4 (c).

Overall, dust particle sizes and deposition fluxes in the lower (3,500 m) sediment traps show less seasonality (the difference between the season with highest average dust flux or coarsest grain size and the season with the lowest fluxes or finest sizes) during both years than in the upper (1,200 m) sediment traps (Figure 3). At the same time, the lower sediment traps tend to show higher fluxes than their upper counterpart during the same year (13M2, 13M4 and 14M4; Figure 3). For the sediment traps at M4, geochemical analyses revealed that lateral input of Amazon-River sediments to the upper trap is minimal, if not absent (Van der Does, Pourmand, et al., 2018), while the lower trap at 13M5 was affected by downslope transport of sediment re-suspended from the nearby Barbados margin, causing much higher deposition fluxes than expected for the overall downwind decreasing trend, including the large outlier in April 2013 (Figure 3; Korte et al., 2020).

3.3. MWAC Samplers

The MWAC samplers that were attached to both buoys collected dust in parallel with the sediment traps at stations M3 and M4 in 2014, but only as a single composite sample over the entire mooring period. Dust collected using these two different sampling methods shows almost identical particle-size distributions (Figures 4b and 4c), although at station M3 the MWAC-sampler shows slightly finer dust than the sediment-trap average (Figure 4b). The grain-size distributions of the seafloor sediments are much finer grained than the dust intercepted in the water column or the atmosphere above, which is due to the much longer timespan these samples represent, of several hundreds of years of sediment accumulation. The secondary mode or "shoulder" of the grain-size distributions is represented in both the MWAC and sediment trap samples, demonstrating the close agreement between the two different sampling methods. Not only the upper traps but also the dust in the lower trap at M4 resembles the atmospheric dust very well. This demonstrates that although modal grain sizes in both the upper and lower traps show differences in seasonality and absolute grain sizes (Figure 3), the average annual grain-size distributions are very similar to the dust collected from the atmosphere directly above. Moreover, dust collected by the MWAC samplers in 2015 also shows the expected downwind-fining trend, with dust collected by buoy M3 being coarser-grained than further downwind by buoy M4 (Figure 5n).

Dust accumulation in the MWAC samplers is very low, ranging from 0.04 to 0.13 mg day^{-1} (Table 1), which is not surprising, given the small opening of the samplers (7.5 mm ∅). In 2014 the difference between the two buoys is very small, however during both sampling years the total dust mass at the more proximal buoy M3 is larger than at the more distal buoy M4.

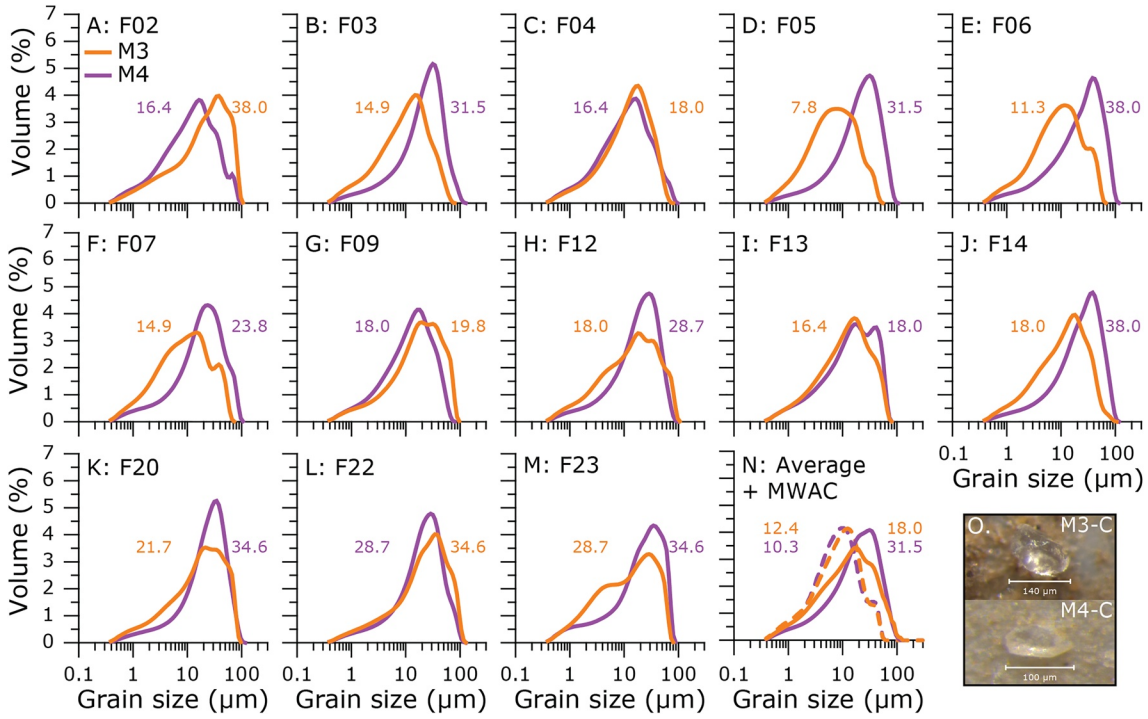

Figure 5. (a–m) Comparison of grain-size distributions between buoy filters (F-nr.) of M3-C (orange) and M4-C (purple) in 2015. (n) Average grain-size distributions of buoys M3 ($N = 14$) and M4 ($N = 20$; solid lines) and the two 2015 Modified Wilson and Cooke (MWAC) samples (dashed lines). The modal grain sizes are included in the plots. (o) Giant dust particles found on buoy filters of M3-C (top) and M4-C (bottom). The sampling periods of the individual filters correspond to the samples of the bar graph shown in Figure 6.

3.4. Buoy Filters

Although all the buoy filters of 2014 (M3-A, B; M4-A) were broken, some still contained enough dust for particle-size analysis, mostly collected during winter (Figure 4a). However, the grain-size distributions are likely biased due to the loss of coarser particles and under-sampling after the filters broke, resulting in irregular and less reliable particle-size distributions. Modal grain sizes range between 2.8 and 5.4 µm (first and main mode), and although fine-grained dust is expected in winter, they are much finer-grained than the finest-grained sediment-trap samples at M3 and M4 (Figure 3). All samples show a secondary mode at ~15 µm. The buoy grain-size distributions show finer-grained dust than that collected by the MWAC samplers in 2014, which sampled for an entire year or even longer (Figure 4a).

In 2015 all buoy filters returned intact, and most contained enough dust for grain-size analysis (Figure 5). Modal grain sizes range between 7.8 and 38.0 µm (average 19.9 µm) for eastern buoy M3-C, and between 14.9 and 38.0 µm (average 24.2 µm) for the more western buoy M4-C. Secondary shoulders in the grain-size distributions are mostly absent, and buoy samples are coarser-grained than the MWAC and sediment trap samples (Figure 4). Giant (>75 µm) quartz particles were found on the filters from both buoys (Figure 5o), which were transported over thousands of kilometres and collected directly from the atmosphere, and which confirms previous findings of such giant particles by Van der Does, Knippertz, et al. (2018). For some samples, dust collected by the more downwind buoy M4 appears to be coarser-grained, but their average grain-size distribution is very similar (Figure 5n).

In contrast to the subsurface sediment traps, the buoys sampled the dust directly from the air, and as a result they register the concentration of dust in the atmosphere, which is a measure for dust *transport*, as opposed to dust *deposition* over the ocean which is registered by the sediment traps. In 2015, an average of 2288 and 5914 L of air were pumped through each filter per day for buoy M3-C and M4-C, respectively. Dust concentrations vary between 6.6 and 51.7 µg m^{-3} (average 19.8 µg m^{-3}) for buoy M3-C, and between 2.5 and 33.0 µg m^{-3} (average 8.2 µg m^{-3}) for buoy M4-C (Figure 6). This downwind decrease in concentration is much more evident than the accompanying grain-size distributions and modal grain sizes (Figure 5). Although there

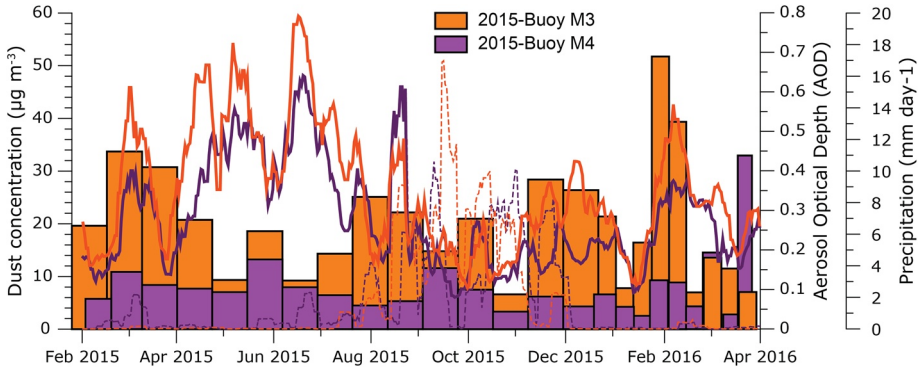

Figure 6. Measured atmospheric dust concentrations (bars) on the 24 buoy filters, aerosol optical depth (AOD, from Moderate Resolution Imaging Spectroradiometer (MODIS) Terra; solid lines) and precipitation (from Tropical Rainfall Measuring Mission (TRMM), dashed lines) for buoys M3-C and M4-C in 2015.

is no clear seasonal signal in dust concentrations over the year for either buoy, the individual peaks match well between the two sites, with a smaller amplitude and absolute concentrations for buoy M4. The dust concentrations also match the satellite-observed atmospheric dust load, represented by the aerosol optical depth for most of the year, except for summer, when atmospheric dust loads are high, but dust concentrations as collected by the buoys are low, in parallel with increased precipitation (Figure 6).

4. Discussion

Dust sampling for this study was carried out using three different methods. First, dust was directly sampled from the atmosphere by the dust-collecting buoys over regular time intervals, revealing dust concentrations during atmospheric transport. Second, passive MWAC samplers attached to these buoys took one discrete sample of atmospheric dust during the entire deployment period of the buoys. Dust entering these samplers by raindrops cannot be excluded entirely since the glass tubes of the samplers do allow rainwater to enter. Third, the subsurface sediment traps collected both dry- and wet-deposited dust continuously at 1,200 and 3,500 m depth along the full transect, synchronously with the dust-collecting buoys at the surface. Combined, these methods show the relationship between atmospheric dust transport and dust deposition.

4.1. Atmospheric Dust: Transport Versus Deposition

There appears to be no clear seasonal trend for neither the atmospheric concentrations of dust nor the particle sizes during atmospheric transport, as sampled by the buoys (Figures 5 and 6). By contrast, dust deposition recorded by the subsurface sediment traps does show a clear seasonal trend of increased fluxes in summer and autumn with coarser-grained dust, and lower deposition fluxes with finer-grained dust in winter and spring. In the summer season, generally more and coarser dust is transported from its north African sources with stronger winds at higher altitudes (Friese et al., 2017), at a maximum altitude of 5–7 km across the Atlantic Ocean (Muhs, 2013, Figure 7; H. Yu et al., 2019). These larger amounts of atmospheric dust are reflected by high AOD values (Figure 6), but most of this dust is above the sampling range of the surface buoys due to the high altitude of SAL transport. In winter, dust transport occurs at lower altitudes (Figure 7), between 0 and 3 km over the eastern Atlantic and between 0 and 2 km over the western Atlantic (Muhs, 2013; Tsamalis et al., 2013), and is more susceptible to dry deposition along the transect (H. Yu et al., 2019). This dust is therefore more readily collected by the surface buoys that sample at sea level. At lower latitudes, wet deposition plays a more important role in winter, due to precipitation related to the ITCZ (H. Yu et al., 2019).

A comparison of dust deposition fluxes in the sediment traps combined with precipitation data from satellites and with model simulations of dust deposition revealed that the main mechanism of dust deposition over the Atlantic Ocean is wet deposition, mostly occurring in summer (Bory et al., 2002; Van der Does et al., 2020). Over the eastern Atlantic, close to the source, dry deposition still plays a significant role, but

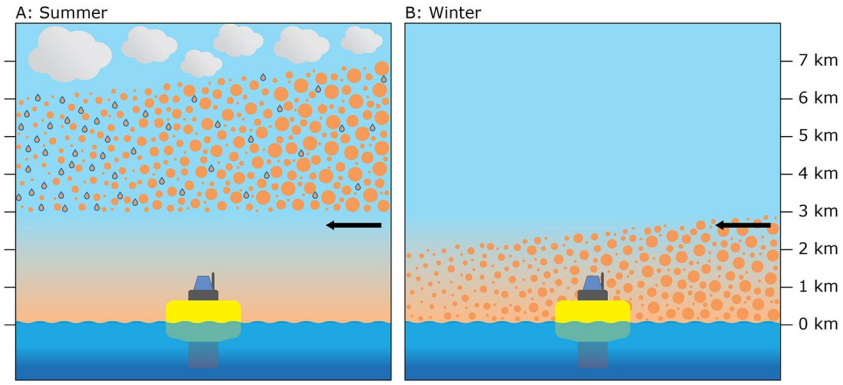

Figure 7. Schematic overview of summer (a) and winter (b) dust transport over the Atlantic Ocean, not to scale. (a) Summer scenario depicting larger amounts and coarser-grained dust by both dry and wet deposition in the east, and lower amounts and finer-grained dust by predominantly wet deposition in the west. Dust transport occurs at high altitudes, up to 7 km. (b) In winter, the main deposition mechanism over the full transect is by dry deposition. Dust transport occurs at lower altitudes, between 0 and 3 km. Also, generally finer dust particles are deposited in winter.

along the downwind transect, wet deposition progressively becomes nearly the sole depositional process (Van der Does et al., 2020), as schematically illustrated in Figure 7. As it appears, precipitation events starting in summer (Figure 6) wash out large amounts of dust from the atmosphere (H. Yu et al., 2019), which are not sampled by the buoys as sampling is halted as soon as rain is detected by their weather sensors. This results in high (wet) deposition fluxes in the sediment traps, while at the same time dust concentrations are low for the buoys at sea level. The onset of precipitation closely matches the sudden decrease in AOD at the buoy sites (Figure 6), implying a complete wash-out of dust from the atmosphere due to wet deposition. As this large increase in (wet) dust deposition is clearly observed in the sediment-trap samples, wet deposition therefore seems to determine the seasonal trend in both the particle size and the deposition flux. In winter and spring, dust deposition mostly happens by dry deposition (Figure 7b).

Although the dust collected by the buoys lack a clear seasonal signal, inter-annual variations are large. Very fine-grained dust was collected in winter 2014 and much coarser-grained dust throughout the entire year 2015 (Figures 4 and 5), which may well be due to the selective loss of (coarse) particles caused by the broken filters in the 2014 sample set. However, the downwind decrease in dust concentrations measured by the buoys during both years is very clear, with larger amounts of atmospheric dust at the more eastern station M3, and lower dust concentrations downwind at M4 as a result of deposition and diffusion between the stations. The accompanying grain-size distributions are much more similar between both stations, and in some individual samples even coarser-grained for the more downwind buoy at M4 (Figure 5). This could be related to the larger volume of air sampled by the buoy at M4, in turn related to the power at which the engine draws air through the filter, which could have increased the number of large particles sampled. Although dust concentrations are corrected for the increased air volume, their grain-size distributions are not. As the design of the buoys is still improving, further testing of the influence of the air volume sampled by the buoy on the grain-size distribution of the collected dust is necessary. Alternatively, the dust collected by the buoy at M4 could contain a larger contribution of giant dust particles at this site (Figure 5o), but this is difficult to quantify as the applied particle-size analysis method does not yield information on the number of particles.

The particle-size distributions of the dust collected by the MWAC samplers show many similarities to the dust collected by the buoys and the subsurface sediment traps. Only the 2014-MWAC sample from buoy M3 is finer-grained than the synchronous sediment-trap samples, and also finer-grained than the MWAC-sample collected farther downwind at M4. This could be due to the fact that the sampling periods were not equal for both MWACs (Table 1). Especially the MWAC-sampler at M4 (Figure 4c) sampled for a longer period (14 months) than the sediment traps (10, 5 months) at the same site. Also, the MWAC sampler at buoy M3 sampled until late August and may have missed most of the coarser-grained dust that is washed down by late-summer rains, although it is not clear how much wet-deposited dust the samplers collect. In addition, the different collection methods—atmospheric dust transport collected by the MWAC samplers with a possible small contribution from raindrops, and both dry- and wet-deposited dust collected by the sediment

traps—can result in differences in particle-size distributions. In 2015 the MWACs show the expected down-wind fining, with coarser-grained dust sampled at M3 and finer-grained dust at M4 (Figure 5). Because of the similarities between the grain-size distributions of the MWAC samplers and the sediment traps, we conclude that the dust sampled directly from the atmosphere is the same as the lithogenic particles captured by sediment traps below, confirming their common aeolian origin.

4.2. Dust Deposition (Sediment Traps)

Seasonal differences in deposition flux (dry and wet deposition combined) and particle size are largest in the sediment traps at M1 at the eastern edge of the transect (Figure 3), as most dust and coarsest-grained particles are deposited closest to the source (Mahowald et al., 2014; Ryder et al., 2013). This agreement between dust mass flux and particle size implies that the coarser-grained dust determines most of the dust flux at the most upwind site. Downwind, the decrease in particle size is accompanied by a decreased seasonal amplitude, which therefore reduces the relationship between deposition flux and particle size. The decrease in seasonality downwind is also the result of the rapid fall-out of coarser particles closer to the source, which leaves a lower variability of particles sizes for deposition at the more downwind stations, as well as a lower influence on the deposition flux of large dust storms coming from the source areas on the African continent.

In addition to the decrease in seasonality downwind, show the upper traps at 1,200 m depth stronger seasonality than the lower sediment traps at 3,500 m depth, for which we propose several hypotheses. First, this observation could be due to the larger catchment area of the deeper traps. As settling particles are potentially displaced by lateral ocean currents, the deeper traps may sample particles which originated from different or additional regions than the upper traps, also called the "statistical funnel" (Siegel & Deuser, 1997; Waniek et al., 2000). Not only will this potentially change the particle flux in the lower traps with respect to the upper ones, but also delay their arrival in the lower traps given the longer settling times. In addition, the lower ocean-current velocities and lower lateral extent of mooring line motion at the depth of the lower traps could have increased the collecting efficiency for the slowest/smallest settling organic aggregates that carry the dust, and thus result in higher fluxes, although current velocities and trap tilt measured at both depths are well below critical levels (Korte et al., 2017). Second, there is a time lag between particle collection of larger versus smaller sizes by the upper and the lower traps, which is related to the differences in sinking velocity between small and larger dust particles. Large and heavy dust particles, such as giant quartz grains observed by Van der Does, Knippertz, et al. (2018) and also on the buoy filters (Figure 5o) will settle individually, but smaller dust particles will only do so agglomerated in marine snow (Van der Jagt et al., 2018), which will take some time to form before settling out. Clemens (1998) argued that the reason for a lacking relation between grain size and particle flux in sediment traps is the larger settling velocities of coarse-grained particles compared to finer-grained ones. This could in turn result in an expression of coarser-grained particles in the sediment traps during large dust storm events, while the associated high dust flux lags behind this signal as finer-grained particles have not yet settled to the sediment trap depth (Clemens, 1998). This effect would be larger at greater depths. In our sediment-trap samples we seem to observe this time-lag effect as the particle size increases before deposition fluxes increase (Figure 3). The same holds for larger/denser marine snow aggregates that settle faster than the smaller/lighter ones, which both carry the finer dust, leading to smoothening of the seasonal signal. Sampling at an even higher resolution should shed more light on the validity of this statement. Third, the deep sediment trap at M5 likely received a large contribution of fine-grained resuspended sediment from the nearby Barbados margin (Korte et al., 2020), either by nepheloid layers (Inthorn, Mohrholz, & Zabel 2006, Inthorn, Wagner, et al., 2006) and/or along-margin transport by ocean currents (Bonnin et al., 2006), leading to increased particle fluxes with depth (Honjo et al., 1982). At M5L (3,500 m BSL), the strong negative correlation between the deposition flux and particle size implies that a larger input of lithogenic material coincided with smaller modal grain sizes. Although the particle size of the lithogenic material collected at this station matches the down-wind fining trend, riverine particles or hemipelagic sediments are also characterized by smaller particle sizes (Filipsson et al., 2011; Holz et al., 2007), and the strong negative relation argues for increased input of such fine-grained sediments. Without a shallow sediment trap to compare, we hypothesize that nonaeolian sediments represent a (significant) contribution to this westernmost deep sediment trap. The other lower sediment traps used in the present study, however, are at a generous distance (880–1,320 m) above the seafloor, while all sediment traps at stations M1–M4 are located much further from continental

margins, where input of laterally transported riverine sediments is shown to be negligible (Van der Does, Pourmand, et al., 2018).

5. Conclusions

We present a unique time series of Saharan dust transport, sampled directly from the atmosphere by surface buoys, and dust deposition, sampled by subsurface sediment traps at two depths along a transect in the tropical North Atlantic Ocean. This study has revealed important insights in the effects of long-range transport and (dry and wet) deposition of mineral dust on the grain-size distributions and deposition fluxes. Results show the high similarity between dust collected during atmospheric transport and the deposition of lithogenic particles collected while sinking to the ocean floor, demonstrating their common aeolian origin. However, they also reveal the differences between dust *transport* on one hand and *deposition* on the other. The subsurface sediment traps collected both dry- and wet-deposited dust, with increased deposition fluxes and coarser grain size in summer and autumn, due to wet deposition by summer rains. In contrast, the surface buoys only sampled dry dust in transport at sea level and lack the clear seasonal signal. This implies that the large amounts of dust transported at high altitudes in summer, brought down by wet deposition, determines the seasonality of both the deposition flux as well as the particle size of the deposited dust. Consequently, satellite observations of atmospheric dust cannot be directly extrapolated to oceanic dust deposition fluxes. The processes involved in dust transport as well as dry and wet deposition have a more complex relationship than previously thought. The sampling transect presented here has been and will be continued for at least several more years, albeit with a different set-up, and future studies will involve the additional wet-deposition sampling by the surface buoys. This study provides important new insights into these processes that can be used for climate model simulations that incorporate dust transport and deposition, and for the interpretation of long-term paleorecords of dust deposition.

Data Availability Statement

Data used in this manuscript are available at https://doi.pangaea.de/10.1594/PANGAEA.922926.

Acknowledgments
This project was funded by grants from NWO (project 822.01.008, TRAFFIC), and ERC (project 311152, DUST-TRAFFIC), both awarded to JBS. The captains, crews, and scientists of FS *Meteor* cruise M89, RV *Pelagia* cruises 64PE378 and 64PE395, RRS *James Cook* cruise JC134, and NIOZ technicians are thanked for deployment and retrieval of the sediment-trap moorings and buoys. NIOZ technicians are also thanked for the design and improvement of the dust-collecting buoys. Chris Munday, Piet van Gaever and Juliane Steinhardt are thanked for their assistance in sediment-trap sample processing. Open access funding enabled and organized by Projekt DEAL.

References

Adams, A. M., Prospero, J. M., & Zhang, C. (2012). CALIPSO-derived three-dimensional structure of aerosol over the Atlantic basin and adjacent continents. *Journal of Climate*, *25*(19), 6862–6879. https://doi.org/10.1175/JCLI-D-11-00672.1

Adebiyi, A. A., & Kok, J. F. (2020). Climate models miss most of the coarse dust in the atmosphere. *Science Advances*, *6*(15), eaaz9507. https://doi.org/10.1126/sciadv.aaz9507

Atkinson, J. D., Murray, B. J., Woodhouse, M. T., Whale, T. F., Baustian, K. J., Carslaw, K. S., et al. (2013). The importance of feldspar for ice nucleation by mineral dust in mixed-phase clouds. *Nature*, *498*(7454), 355–358. https://doi.org/10.1038/nature12278

Baker, A. R., Lesworth, T., Adams, C., Jickells, T. D., & Ganzeveld, L. (2010). Estimation of atmospheric nutrient inputs to the Atlantic Ocean from 50°N to 50°S based on large-scale field sampling: Fixed nitrogen and dry deposition of phosphorus. *Global Biogeochemical Cycles*, *24*, GB3006. https://doi.org/10.1029/2009GB003634

Bale, N. (2014). *Cruise Report RV Pelagia 64PE393, HCC cruise. 26 August–21 September 2014*. Retreived from http://melia.nioz.nl/public/dmg/rpt/crs/64pe393.pdf

Ben-Ami, Y., Koren, I., Altaratz, O., Kostinski, A., & Lehahn, Y. (2012). Discernible rhythm in the spatio/temporal distributions of transatlantic dust. *Atmospheric Chemistry and Physics*, *12*(5), 2253–2262. https://doi.org/10.5194/acp-12-2253-2012

Bergametti, G., & Forêt, G. (2014). Dust Deposition. In P. Knippertz, & J. B. W. stuut (Eds.), *Mineral dust, A key player in the Earth system, springer* (pp. 179–200) (ISBN: 978-94-017-8977-6). https://doi.org/10.1007/978-94-017-8978-3_8

Bonnin, J., Van Haren, H., Hosegood, P., & Brummer, G.-J. A. (2006). Burst resuspension of seabed material at the foot of the continental slope in the Rockall Channel. *Marine Geology*, *226*(3), 167–184. https://doi.org/10.1016/j.margeo.2005.11.006

Bory, A., Dulac, F., Moulin, C., Chiapello, I., Newton, P. P., Guelle, W., et al. (2002). Atmospheric and oceanic dust fluxes in the northeastern tropical Atlantic Ocean: How close a coupling? *Annales Geophysicae*, *20*(12), 2067–2076. https://doi.org/10.5194/angeo-20-2067-2002

Brust, J., Schulz-Bull, D. E., Leipe, T., Chavagnac, V., & Waniek, J. J. (2011). Descending particles: From the atmosphere to the deep ocean—A time series study in the subtropical NE Atlantic. *Geophysical Research Letters*, *38*, L06603. https://doi.org/10.1029/2010GL045399

Clemens, S. C. (1998). Dust response to seasonal atmospheric forcing: Proxy evaluation and calibration. *Paleoceanography*, *13*(5), 471–490. https://doi.org/10.1029/98PA02131

Filipsson, H. L., Romero, O. E., Stuut, J. B. W., & Donner, B. (2011). Relationships between primary productivity and bottom-water oxygenation off northwest Africa during the last deglaciation. *Journal of Quaternary Science*, *26*(4), 448–456. https://doi.org/10.1002/jqs.1473

Fischer, G., Romero, O., Merkel, U., Donner, B., Iversen, M., Nowald, N., et al. (2016). Deep ocean mass fluxes in the coastal upwelling off Mauritania from 1988 to 2012: Variability on seasonal to decadal timescales. *Biogeosciences*, *13*(10), 3071–3090. https://doi.org/10.5194/bg-13-3071-2016

Fomba, K. W., Müller, K., van Pinxteren, D., Poulain, L., van Pinxteren, M., & Herrmann, H. (2014). Long-term chemical characterization of tropical and marine aerosols at the Cape Verde Atmospheric Observatory (CVAO) from 2007 to 2011. *Atmospheric Chemistry and Physics*, *14*(17), 8883–8904. https://doi.org/10.5194/acp-14-8883-2014

Friese, C. A., van der Does, M., Merkel, U., Iversen, M. H., Fischer, G., & Stuut, J.-B. W. (2016). Environmental factors controlling the seasonal variability in particle size distribution of modern Saharan dust deposited off Cape Blanc. *Aeolian Research*, *22*, 165–179. https://doi.org/10.1016/j.aeolia.2016.04.005

Friese, C. A., van Hateren, J. A., Vogt, C., Fischer, G., & Stuut, J. B. W. (2017). Seasonal provenance changes in present-day Saharan dust collected in and off Mauritania. *Atmospheric Chemistry and Physics*, *17*(16), 10163–10193. https://doi.org/10.5194/acp-17-10163-2017

Goossens, D., & Offer, Z. Y. (2000). Wind tunnel and field calibration of six aeolian dust samplers. *Atmospheric Environment*, *34*(7), 1043–1057. https://doi.org/10.1016/S1352-2310(99)00376-3

Goossens, D., Offer, Z., & London, G. (2000). Wind tunnel and field calibration of five aeolian sand traps. *Geomorphology*, *35*(3–4), 233–252. https://doi.org/10.1016/S0169-555X(00)00041-6

Goudie, A. S., & Middleton, N. J. (2001). Saharan dust storms: Nature and consequences. *Earth-Science Reviews*, *56*(1–4), 179–204. https://doi.org/10.1016/S0012-8252(01)00067-8

Guerreiro, C. V., Baumann, K. H., Brummer, G. J. A., Fischer, G., Korte, L. F., Merkel, U., et al. (2017). Coccolithophore fluxes in the open tropical North Atlantic: Influence of thermocline depth, Amazon water, and Saharan dust. *Biogeosciences*, *14*(20), 4577–4599. https://doi.org/10.5194/bg-14-4577-2017

Holz, C., Stuut, J. B. W., & Henrich, R. (2004). Terrigenous sedimentation processes along the continental margin off NW Africa: Implications from grain-size analysis of seabed sediments. *Sedimentology*, *51*(5), 1145–1154. https://doi.org/10.1111/j.1365-3091.2004.00665.x

Holz, C., Stuut, J. B. W., HenrIch, R., & Meggers, H. (2007). Variability in terrigenous sedimentation processes off Northwest Africa and its relation to climate changes: Inferences from grain-size distributions of a Holocene marine sediment record. *Sedimentary Geology*, *202*(3), 499–508. https://doi.org/10.1016/j.sedgeo.2007.03.015

Honjo, S., Manganini, S. J., & Poppe, L. J. (1982). Sedimentation of lithogenic particles in the deep ocean. *Marine Geology*, *50*(3), 199–220. https://doi.org/10.1016/0025-3227(82)90139-6

Inthorn, M., Mohrholz, V., & Zabel, M. (2006). Nepheloid layer distribution in the Benguela upwelling area offshore Namibia: Deep Sea Research Part I. *Oceanographic Research Papers*, *53*(8), 1423–1438. https://doi.org/10.1016/j.dsr.2006.06.004

Inthorn, M., Wagner, T., Scheeder, G., & Zabel, M. (2006). Lateral transport controls distribution, quality, and burial of organic matter along continental slopes in high-productivity areas. *Geology*, *34*(3), 205–208. https://doi.org/10.1130/G22153.1

Kandler, K., Schütz, L., Deutscher, C., Ebert, M., Hofmann, H., JÄCkel, S., et al. (2009). Size distribution, mass concentration, chemical and mineralogical composition and derived optical parameters of the boundary layer aerosol at Tinfou, Morocco, during SAMUM 2006. *Tellus B: Chemical and Physical Meteorology*, *61*(1), 32–50. https://doi.org/10.1111/j.1600-0889.2008.00385.x

Kok, J. F., Adebiyi, A. A., Albani, S., Balkanski, Y., Checa-Garcia, R., Chin, M., et al. (2020). Improved representation of the global dust cycle using observational constraints on dust properties and abundance. *Atmospheric Chemistry and Physics*, 1–45. https://doi.org/10.5194/acp-2020-1131

Korte, L. F., Brummer, G. J. A., van der Does, M., Guerreiro, C. V., Hennekam, R., van Hateren, J. A., et al. (2017). Downward particle fluxes of biogenic matter and Saharan dust across the equatorial North Atlantic: Atmos. *Chemical Physics*, *17*(9), 6023–6040. https://doi.org/10.5194/acp-17-6023-2017

Korte, L. F., Brummer, G. J. A., van der Does, M., Guerreiro, C. V., Mienis, F., Munday, C. I., et al. (2020). Multiple drivers of production and particle export in the western tropical North Atlantic. *Limnology & Oceanography*, *65*, 2108–2124. https://doi.org/10.1002/lno.11442

Korte, L. F., Pausch, F., Trimborn, S., Brussaard, C. P. D., Brummer, G. J. A., van der Does, M., et al. (2018). Effects of dry and wet Saharan dust deposition in the tropical North Atlantic Ocean. *Biogeosciences Discussions*, *2018*, 1–20. https://doi.org/10.5194/bg-2018-484

Mahowald, N., Albani, S., Kok, J. F., Engelstaeder, S., Scanza, R., Ward, D. S., & Flanner, M. G. (2014). The size distribution of desert dust aerosols and its impact on the earth system. *Aeolian Research*, *15*, 53–71. https://doi.org/10.1016/j.aeolia.2013.09.002

Marticorena, B. (2014). Dust production mechanisms. In P. Knippertz, & J. B. W. Stuut (Eds.). *Mineral dust, A key player in the earth system*, (pp. 93–120) (ISBN: 978-94-017-8977-6). Springer. https://doi.org/10.1007/978-94-017-8978-3_5

Marticorena, B., Chatenet, B., Rajot, J. L., Traore, S., Coulibaly, M., Diallo, A., et al. (2010). Temporal variability of mineral dust concentrations over West Africa: Analyses of a pluriannual monitoring from the AMMA Sahelian Dust Transect. *Atmospheric Chemistry and Physics*, *10*(18), 8899–8915. https://doi.org/10.5194/acp-10-8899-2010

Meskhidze, N., Chameides, W. L., & Nenes, A. (2005). Dust and pollution: A recipe for enhanced ocean fertilization? *Journal of Geophysical Research*, *110*, D03301. https://doi.org/10.1029/2004jd005082

Mills, M. M., Ridame, C., Davey, M., La Roche, J., & Geider, R. J. (2004). Iron and phosphorus co-limit nitrogen fixation in the eastern tropical North Atlantic. *Nature*, *429*, 292–294. https://doi.org/10.1038/nature02550

Muhs, D. R. (2013). The geologic records of dust in the Quaternary. *Aeolian Research*, *9*, 3–48. https://doi.org/10.1016/j.aeolia.2012.08.001

Nicholson, S. E. (2000). The nature of rainfall variability over Africa on time scales of decades to millenia. *Global and Planetary Change*, *26*(1–3), 137–158. https://doi.org/10.1016/S0921-8181(00)00040-0

Nowald, N., Iversen, M. H., Fischer, G., Ratmeyer, V., & Wefer, G. (2015). Time series of in-situ particle properties and sediment trap fluxes in the coastal upwelling filament off Cape Blanc. *Mauritania: Progress in Oceanography*, *137*, 1–11. https://doi.org/10.1016/j.pocean.2014.12.015

Pabortsava, K., Lampitt, R. S., Benson, J., Crowe, C., McLachlan, R., Le Moigne, F. A. C., et al. (2017). Carbon sequestration in the deep Atlantic enhanced by Saharan dust. *Nature Geoscience*, *10*, 189–194. https://doi.org/10.1038/ngeo2899

Prospero, J. M., Collard, F.-X., Molinié, J., & Jeannot, A. (2014). Characterizing the annual cycle of African dust transport to the Caribbean Basin and South America and its impact on the environment and air quality. *Global Biogeochemical Cycles*, *28*(7), 757–773. https://doi.org/10.1002/2013GB004802

Prospero, J. M., Landing, W. M., & Schulz, M. (2010). African dust deposition to Florida: Temporal and spatial variability and comparisons to models. *Journal of Geophysical Research*, *115*, D13304. https://doi.org/10.1029/2009JD012773

Ridame, C., Dekaezemacker, J., Guieu, C., Bonnet, S., L'Helguen, S., & Malien, F. (2014). Contrasted Saharan dust events in LNLC environments: Impact on nutrient dynamics and primary production. *Biogeosciences*, *11*(17), 4783–4800. https://doi.org/10.5194/bg-11-4783-2014

Ryder, C. L., Highwood, E. J., Rosenberg, P. D., Trembath, J., Brooke, J. K., Bart, M., et al. (2013). Optical properties of Saharan dust aerosol and contribution from the coarse mode as measured during the Fennec 2011 aircraft campaign. *Atmospheric Chemistry and Physics*, *13*(1), 303–325. https://doi.org/10.5194/acp-13-303-2013

Ryder, C. L., Highwood, E. J., Walser, A., Seibert, P., Philipp, A., & Weinzierl, B. (2019). Coarse and giant particles are ubiquitous in Saharan dust export regions and are radiatively significant over the Sahara. *Atmospheric Chemistry and Physics*, *19*(24), 15353–15376. https://doi.org/10.5194/acp-19-15353-2019

Sarnthein, M., Tetzlaff, G., Koopmann, B., Wolter, K., & Pflaumann, U. (1981). Glacial and interglacial wind regimes over the Eastern Subtropical Atlantic and North-West Africa. *Nature*, *293*(5829), 193–196. https://doi.org/10.1038/293193a0

Schlitzer, R. (2018). *Ocean data view*. Retrieved from https://odv.awi.de

Sholkovitz, E., Allsup, G., Hosom, D., & Purcell, M. (2001). An autonomous aerosol sampler/elemental analyzer designed for ocean buoys and remote land sites. *Atmospheric Environment*, *35*(16), 2969–2975. https://doi.org/10.1016/S1352-2310(01)00068-1

Sholkovitz, E. R., & Sedwick, P. N. (2006). Open-ocean deployment of a buoy-mounted aerosol sampler on the Bermuda testbed mooring: Aerosol iron and sea salt over the Sargasso Sea: Deep Sea Research Part I. *Oceanographic Research Papers*, *53*(3), 547–560. https://doi.org/10.1016/j.dsr.2005.12.002

Siegel, D. A., & Deuser, W. G. (1997). Trajectories of sinking particles in the Sargasso Sea: Modeling of statistical funnels above deep-ocean sediment traps. *Deep Sea Research Part I: Oceanographic Research Papers*, *44*(9–10), 1519–1541. https://doi.org/10.1016/S0967-0637(97)00028-9

Skonieczny, C., Bory, A., Bout-Roumazeilles, V., Abouchami, W., Galer, S. J. G., Crosta, X., et al. (2013). A three-year time series of mineral dust deposits on the West African margin: Sedimentological and geochemical signatures and implications for interpretation of marine. *Paleo-Dust Records: Earth and Planetary Science Letters*, *364*(0), 145–156. https://doi.org/10.1016/j.epsl.2012.12.039

Stuut, J. B., Boekschoten, B., Boersen, B., Brummer, G. J., Brussaard, C., de Boer, J., et al. (2016). *Cruise Report RRS James Cook JC134, TRAFFIC IV: Transatlantic Fluxes of Saharan Dust. 19 March - 16 April 2016*. Retrieved from http://melia.nioz.nl/public/dmg/rpt/crs/JC134.pdf

Stuut, J. B., Boersen, B., Brück, H. M., Hansen, A., Koster, B., van der Does, M., & Witte, Y. (2012). *Cruise Report RV Meteor M89, TRAFFIC I: Transatlantic Fluxes of Saharan Dust. 3 - 25 October 2012*. Retrieved from http://melia.nioz.nl/public/dmg/rpt/crs/m89.pdf

Stuut, J. B., Brummer, G. J. A., van der Does, M., Friese, C., Geerken, E., van der Heide, R., et al. (2013). *Cruise Report RV Pelagia 64PE378, TRAFFIC II: Transatlantic Fluxes of Saharan Dust. 9 November - 6 December 2013*. Retrieved from http://melia.nioz.nl/public/dmg/rpt/crs/64pe378.pdf

Stuut, J. B., Witte, Y., de Visser, J.-D., Boersen, B., Koster, B., Bakker, K., et al. (2015). *Cruise Report RV Pelagia 64PE395, TRAFFIC III: Transatlantic Fluxes of Saharan Dust. 11 January - 6 February 2015*. Retrieved from http://melia.nioz.nl/public/dmg/rpt/crs/64pe395.pdf

Stuut, J. B., Zabel, M., Ratmeyer, V., Helmke, P., Schefuss, E., Lavik, G., & Schneider, R. (2005). Provenance of present-day eolian dust collected off NW Africa. *Journal of Geophysical Research*, *110*, D04202. https://doi.org/10.1029/2004JD005161

Tsamalis, C., Chedin, A., Pelon, J., & Capelle, V. (2013). The seasonal vertical distribution of the Saharan Air Layer and its modulation by the wind. *Atmospheric Chemistry and Physics*, *13*(22), 11235–11257. https://doi.org/10.5194/acp-13-11235-2013

Twohy, C. H., Kreidenweis, S. M., Eidhammer, T., Browell, E. V., Heymsfield, A. J., Bansemer, A. R., et al. (2009). Saharan dust particles nucleate droplets in eastern Atlantic clouds. *Geophysical Research Letters*, *36*, L01807. https://doi.org/10.1029/2008GL035846

van der Does, M., Brummer, G.-J. A., Van Crimpen, F. C. J., Korte, L. F., Mahowald, N. M., Merkel, U., et al. (2020). Tropical rains controlling deposition of saharan dust across the north atlantic ocean. *Geophysical Research Letters*, *47*, e2019GL086867. https://doi.org/10.1029/2019GL086867

Van der Does, M., Knippertz, P., Zschenderlein, P., Giles Harrison, R., & Stuut, J.-B. W. (2018). The mysterious long-range transport of giant mineral dust particles. *Science Advances*, *4*(12), eaau2768. https://doi.org/10.1126/sciadv.aau2768

Van der Does, M., Korte, L. F., Munday, C. I., Brummer, G. J. A., & Stuut, J. B. W. (2016). Particle size traces modern Saharan dust transport and deposition across the equatorial North Atlantic: Atmos. *Chemical Physics*, *16*(21), 13697–13710. https://doi.org/10.5194/acp-16-13697-2016

Van der Does, M., Pourmand, A., Sharifi, A., & Stuut, J. B. W. (2018). North African mineral dust across the tropical Atlantic Ocean: Insights from dust particle size, radiogenic Sr-Nd-Hf isotopes and rare earth elements (REE). *Aeolian Research*, *33*, 106–116. https://doi.org/10.1016/j.aeolia.2018.06.001

Van der Jagt, H., Friese, C., Stuut, J. B., Fischer, G., & Iversen, M. (2018). The ballasting effect of Saharan dust deposition on aggregate dynamics and carbon export: Aggregation, settling and scavenging of marine snow. *Limnology & Oceanography*, *63*, 1386–1394. https://doi.org/10.1002/lno.10779

Waniek, J., Koeve, W., & Prien, R. D. (2000). Trajectories of sinking particles and the catchment areas above sediment traps in the northeast Atlantic. *Journal of Marine Research*, *58*(6), 983–1006. https://doi.org/10.1357/002224000763485773

Weinzierl, B., Ansmann, A., Prospero, J. M., Althausen, D., Benker, N., Chouza, F., et al. (2017). The Saharan aerosol long-range transport and aerosol–cloud-interaction experiment: Overview and selected highlights. *Bulletin of the American Meteorological Society*, *98*(7), 1427–1451. https://doi.org/10.1175/BAMS-D-15-00142.1

Yu, H., Chin, M., Yuan, T., Bian, H., Remer, L. A., Prospero, J. M., et al. (2015). The fertilizing role of African dust in the Amazon rainforest: A first multiyear assessment based on data from Cloud-Aerosol Lidar and Infrared Pathfinder Satellite Observations. *Geophysical Research Letters*, *42*, 1984–1991. https://doi.org/10.1002/2015GL063040

Yu, H., Tan, Q., Chin, M., Remer, L. A., Kahn, R. A., Bian, H., et al. (2019). Estimates of African dust deposition along the trans-Atlantic transit using the decadelong record of aerosol measurements from CALIOP, MODIS, MISR, and IASI. *Journal of Geophysical Research: Atmospheres*, *124*, 7975–7996. https://doi.org/10.1029/2019jd030574

Yu, Y., Kalashnikova, O. V., Garay, M. J., Lee, H., Notaro, M., Campbell, J. R., et al. (2020). Disproving the Bodélé depression as the primary source of dust fertilizing the Amazon Rainforest. *Geophysical Research Letters*, *47*, e2020GL088020. https://doi.org/10.1029/2020GL088020

Zender, C. S., Bian, H., & Newman, D. (2003). Mineral Dust Entrainment and Deposition (DEAD) model: Description and 1990s dust climatology. *Journal of Geophysical Research*, *108*, 4416. https://doi.org/10.1029/2002JD002775